PHYSICAL REVIEW B VOLUME 27, NUMBER 7 1 APRIL 1983

Double electron-muon resonance experiments on muonium in quartz

J. A. Brown, R. H. Heffner, and M. Leon
Los Alamos National Laboratory, Los Alamos, New Mexico 87545

S. A. Dodds, T. L. Estle, and D. A. Vanderwater*
Rice University, Houston, Texas 77251
(Received 2 September 1982)

Double electron-muon resonance experiments on muonium in quartz are described. The observed muon-spin—rotation spectra show a structure resulting from the coherent response of the system to the radio-frequency magnetic field. The theory of this structure is developed and agreement with experiment is within experimental error.

I. INTRODUCTION

A positive muon implanted in a semiconductor or insulator often binds an electron to form a muoniumlike defect center. Usually these centers are very similar to muonium in vacuum, hence they have large hyperfine splittings. However, in the group-IV crystals, diamond, silicon, and germanium, a defect center called anomalous muonium is observed to have a very small hyperfine interaction (which is also very anisotropic). Any of these muoniumlike defects can be studied by muon-spin rotation (μSR).[1-3] This technique allows one to deduce the time history of the muon-spin precession by observation of the muon-decay positrons. The type of information obtainable from μSR studies is similar to that found from nuclear-magnetic-resonance (NMR) or electron-paramagnetic-resonance (EPR) studies on stable defect centers. However, the μSR spectrum corresponds to observation of allowed magnetic dipole transitions of the muon spin. In magnetic fields large enough to decouple the electron and muon spin, i.e., the Paschen-Bach region, electronic magnetic dipole transitions are not seen and consequently there is little information obtained about the electronic Zeeman interaction or nuclear hyperfine coupling to surrounding nuclei. Since the bulk of the μSR data on anomalous muonium is obtained in this high-field limit, this information, which may be quite valuable in constructing and testing models of anomalous muonium, is not readily available. In this paper we describe and demonstrate a new technique which can be elaborated to observe EPR transitions which do not appear directly in the μSR spectrum. These transitions should provide the information not observable by μSR alone.

This paper concerns the effects of a large radio-frequency magnetic field at a frequency near resonance with a magnetic dipole transition of the electron spin. The EPR spectrum can be deduced because of the structure produced in the μSR spectrum and its dependence on the frequency and amplitude of the applied field. The analogy to electron nuclear double resonance (ENDOR) and other double-resonance techniques is apparent, leading to the name double electron-muon resonance (DEMUR). Because the radio-frequency field is large and relaxation is slow the coupled electron-spin—muon-spin system follows the field coherently. These coherence effects produce structure in the μSR spectrum which can be used to locate the EPR transitions. Although this paper demonstrates DEMUR using muonium, and in muonium the allowed electronic and muonic magnetic dipole transitions are identical, the relative ease of the observation of coherence effects together with the variety of experimental circumstances under which they occur makes the study of DEMUR in muonium a goal in itself.

The basic phenomenon can be understood by considering a spin-$\frac{1}{2}$ system subject to a strong radio-frequency field of amplitude H_1 perpendicular to a much larger static field $\vec{H}$. When the frequency is adjusted to be on resonance, the spin will simply precess about the properly rotating component of amplitude $\frac{1}{2}H_1$ in the rotating frame with precessional frequency $\frac{1}{2}\gamma H_1$. A measurement of spin polarization transverse to $\vec{H}$ in the laboratory frame then will show three frequencies: γH and $\gamma H \pm \frac{1}{2}\gamma H_1$.

Muonium is, of course, not a two-level system. The two coupled spin-$\frac{1}{2}$ particles lead to the standard[1,2] Breit-Rabi diagram of Fig. 1 which defines our notation for the energy levels. A complete cal-

culation summarized below and set forth in a companion paper,[4] demonstrates that the qualitative result for a two-level system applies to the driven transition in muonium also. If the allowed transitions are well separated rf can be applied near only one transition frequency. That line in the μSR spectrum will split into three components, as for the spin-$\frac{1}{2}$ example. Other transitions which share an energy level with the driven transition will split into two frequency components. Transitions without a level in common with the driven transition remain unaffected.

This paper presents an experimental test of DEMUR. In this demonstration of DEMUR we chose a system, muonium at moderate field and moderate frequency, in which the allowed magnetic dipole transitions for the muon spin and the electron spin are the same. We thus anticipate coherence effects when the radio frequency is near one of the two μSR frequencies. We have chosen to use muonium in quartz for several reasons: the μSR spectrum is strong and nearly isotropic, all the parameters of the system are known,[5,6] and spin relaxation is negligible. It is therefore possible to predict the DEMUR spectrum exactly for this simple system. Our experimental apparatus and qualitative results are described in the next section. A detailed comparison with the calculated spectrum is provided in Sec. III followed by conclusions in Sec. IV. Preliminary reports of this work have appeared previously.[7,8]

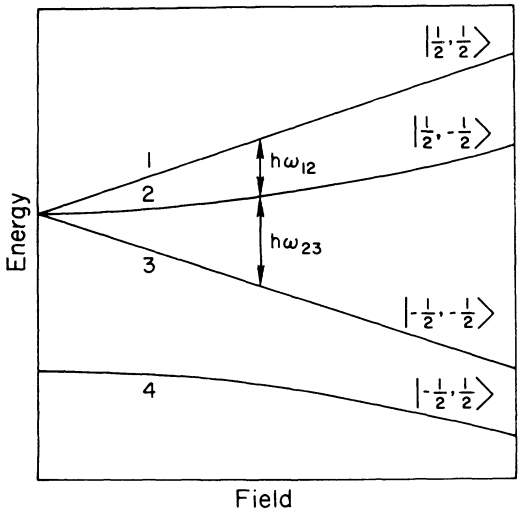

FIG. 1. Breit-Rabi diagram for muonium in quartz. High-field states are labeled with $|M_s,M_I\rangle$, and the observable low-frequency μSR transitions are indicated. Levels 1 and 2 cross at sufficiently high field.

II. EXPERIMENTAL PROCEDURE AND RESULTS

The experiment was performed at the Stopped Muon Channel of the Clinton P. Anderson Meson Physics Facility at Los Alamos National Laboratory (LAMPF). A positive-muon beam with momentum 80 MeV/c and approximately 90% polarization was used with a μSR spectrometer of conventional design.[2] Two positron telescopes were placed outside the beam to detect positrons emitted in a direction perpendicular to both the initial polarization and the static field. The system time resolution was 2 nsec. A pair of coils provided the static magnetic field perpendicular to the initial polarization direction. This field was uniform over the sample volume to about $1{:}10^5$ and stable to $1{:}10^4$ during each measurement.

The radio-frequency magnetic field was produced by the circuit shown in Fig. 2. A three-turn secondary coil was wound directly on the sample and brought to resonance with an adjustable air-dielectric capacitor. The secondary was inductively coupled to a series-tuned coil, driven by a stable oscillator and a 40-W broad-band amplifier. The overall Q was about 200, and the circuit could be tuned from 150 to 190 MHz. The rf phase was random with respect to the muon arrival time. The rf amplitude was monitored with a pickup coil and held constant to 5% or better during a measurement. The maximum amplitude available was about

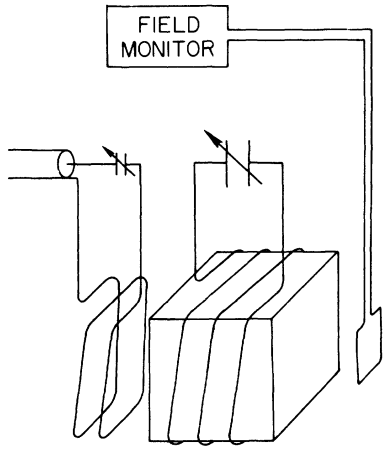

FIG. 2. Diagram of the circuit used to generate the large rf magnetic fields necessary for the DEMUR experiment in quartz.

1.6 G as determined from the DEMUR splittings; no line broadening attributable to rf-field inhomogeneity was observed.

The quartz sample was a synthetically grown single crystal in the form of a 2.5-cm cube. The secondary coil was wound so that the rf magnetic field $\vec{H}_1$ was parallel to the crystal c axis. The coil and sample could then be placed in the apparatus so that $\vec{H}_1$ was either parallel or perpendicular to the initial muon polarization, but always perpendicular to the static field. All measurements were carried out at room temperature.

Time-differential μSR data were obtained over a 1.6-μsec range for several rf frequencies, amplitudes, and orientations. A total of one to four million events were recorded in each of the two histograms for each set of operating conditions. The data were analyzed by Fourier transformation to find approximate peak-frequency positions and amplitudes. More precise frequencies and amplitudes were derived by fitting each time spectrum to the expression

$$N(t)=N_0 e^{-t/\tau_\mu}\left[1+\sum_i a_i\cos(\omega_i t+\phi_i)\right]+B\ . \tag{1}$$

Here N_0 is a scale factor, B is the background (assumed flat), and τ_μ is the muon lifetime. The parameters a_i, ω_i and ϕ_i specify the amplitude, frequency, and phase, respectively, of each frequency component. Relaxation effects were unimportant and were neglected. The parameters of Eq. (1) were adjusted for the best least-squares fit to each histogram, using up to five frequency components for muonium and one for the free-muon signal. Parameters derived from the two histograms were then combined. All errors quoted are one standard deviation for the combined parameters. The results obtained from fits using Eq. (1) and from Fourier transforms agree within errors.

Figures 3 and 4 display data for a constant external field of 124.8 G and several different rf frequencies. The external field, rf field, and initial muon polarization were chosen to be mutually perpendicular. Data were also obtained with $\vec{H}_1$ parallel to the muon polarization but are not shown because they are identical to the $\vec{H}_1$ perpendicular case as expected when the rf phase is uncorrelated with the muon stopping time.

For the data shown in Fig. 3, the rf frequency was set near ω_{23} (180.4 MHz), the midpoint, and near ω_{12} (167.2 MHz). When the applied frequency is near either ω_{12} or ω_{23} that line splits into a triplet. The other transition, which shares level 2 with the driven one, splits into a doublet. When the rf is

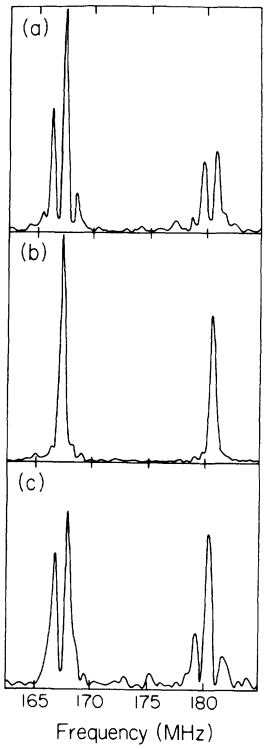

FIG. 3. Results of DEMUR on quartz. These three Fourier power spectra show the effects of applying an rf magnetic field at (a) 167.30 MHz near the lower μSR frequency, (b) 173.90 MHz near the midfrequency point, and (c) 180.51 MHz near the upper μSR transition frequency. For all three sets of data, the dc magnetic field was 124.8 and the rf magnetic field was held at 1.0 G amplitude.

midway between ω_{12} and ω_{23} the spectrum is experimentally indistinguishable from that without rf. The numerical solution discussed in Sec. III shows that in this case the spectrum is composed of two unresolved doublets plus a line at the rf frequency which is too weak to observe.

The results of a more detailed examination of frequencies near resonance are presented in Fig. 4. Using the largest available rf amplitude, the frequency was set in turn very slightly below ω_{23}, very slightly above ω_{23}, and then about 1 MHz above ω_{23} for Figs. 4(a)—4(c). The relative amplitude of the doublet lines is clearly a sensitive detector of the resonance condition. Even if the transition at ω_{23} were not visible in the μSR spectrum, it could be located quite accurately by examining the doublet induced near ω_{12}.

III. QUANTITATIVE ANALYSIS

The data presented in Sec. II can be analyzed in detail using the results of a companion paper.[4] Since that treatment is quite general and therefore

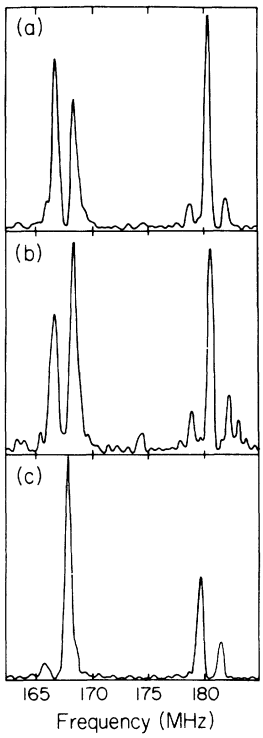

FIG. 4. Results of DEMUR on quartz. The three power spectra shown here were taken with the rf near the upper resonance frequency and (a) slightly below resonance, (b) slightly above resonance, and (c) approximately 1 MHz above resonance. Effect on the relative amplitude of the doublet lines is clearly shown. For all three spectra, $H=124.8$ G and $H_1=1.6$ G.

complicated we present here an abbreviated derivation of the needed equations using the simplifications appropriate to muonium in quartz.

The spin Hamiltonian appropriate for muonium in quartz is

$$\mathscr{H}_0=g\mu_B\vec{H}\cdot\vec{S}-g_\mu\mu_\mu\vec{H}\cdot\vec{I}+A\vec{I}\cdot\vec{S}\ . \tag{2}$$

The g factors and the hyperfine coupling constant A are taken to be isotropic. (The small anisotropy[5] of A is accounted for by treating A as a field-dependent parameter.[6] For $H\approx 125$ G, $A\simeq 4634$ MHz.) In agreement with observation we neglect nuclear hyperfine couplings and relaxation effects.

For a static field H the solutions of Eq. (2) are well known[1,2]; the resulting energy levels are shown in Fig. 1 labeled with the high-field values of $|M_s,M_J\rangle$. In a DEMUR experiment there is an rf field $\vec{H}_1\cos(\omega t+\phi)$ which can cause transitions among these levels. This implies a time-varying contribution

$$\mathscr{H}_1=(g\mu_B\vec{H}_1\cdot\vec{S}-g_\mu\mu_\mu\vec{H}_1\cdot\vec{I})\cos(\omega t+\phi) \tag{3}$$

to the Hamiltonian. The time-dependent solutions of the total Hamiltonian $\mathscr{H}=\mathscr{H}_0+\mathscr{H}_1$ are denoted $\Psi(t)$ and the observable muon polarization at time t is given by

$$\vec{P}(t)=2\langle\Psi(t)\,|\,\vec{I}\,|\,\Psi(t)\rangle\ . \tag{4}$$

Note that since the effects of $\mathscr{H}_1$ are much larger than those from relaxation, a perturbative solution is not appropriate.

If the eigenfunctions and energy levels of $\mathscr{H}_0$ are ψ_n and $\hbar\omega_n$ for $n=1$—4, we can write

$$\Psi(t)=\sum_n a_n(t)\psi_n e^{-i\omega_n t}\ . \tag{5}$$

Inserting $\Psi(t)$ into the time-dependent Schrödinger equation gives a set of coupled equations for the $a_n(t)$,

$$\frac{da_n}{dt}=-i\sum_m a_m(t)\Omega_{nm}e^{i\omega_{nm}t}\cos(\omega t+\phi)\ , \tag{6}$$

where $\omega_{nm}=\omega_n-\omega_m$ and

$$\hbar\Omega_{nm}=\langle\psi_n\,|\,g\mu_B\vec{H}_1\cdot\vec{S}-g_\mu\mu_\mu\vec{H}_1\cdot\vec{I})\,|\,\psi_m\rangle\ . \tag{7}$$

Note that $|\Omega_{nm}|$ is proportional to the rf-field magnitude $|\vec{H}_1|$. The initial conditions are specified by

$$a_n(0)=\langle\psi_n\,|\,\Psi(0)\rangle\ , \tag{8}$$

with $\Psi(0)$ the wave function at $t=0$. To fix $\Psi(0)$, we assume that the electrons are unpolarized and the muons are completely polarized along the beam direction. Equation (6) can be simplified by noting that terms involving level 4 oscillate at high frequency and hence usually cannot be observed. The remaining equations can only be solved numerically unless further approximations are made.

If, as is the case for quartz in moderate fields, the allowed transition frequencies are well separated, it is possible to proceed analytically. Suppose the rf ω is chosen to be near ω_{12}, in the sense that

$$|\omega-\omega_{12}|\lesssim|\Omega_{12}|\ , \tag{9}$$

$$|\omega+\omega_{12}|\gg|\Omega_{12}|\ , \tag{10}$$

$$|\omega\pm\omega_{ij}|\gg|\Omega_{ij}|\quad(i,j\neq 1,2)\ . \tag{11}$$

Retaining only the near-secular terms, Eq. (6) reduces to

$$\frac{da_4}{dt}=\frac{da_3}{dt}=0\ , \tag{12}$$

$$\frac{da_2}{dt}=-\frac{i}{2}\Omega_{12}^{*}a_1 e^{i(\omega-\omega_{12})t}e^{i\phi}\ , \tag{13}$$

$$\frac{da_1}{dt}=-\frac{i}{2}\Omega_{12}a_2 e^{-i(\omega-\omega_{12})t}e^{-i\phi}\ . \tag{14}$$

A similar set of equations would be obtained if ω were chosen to be near ω_{23}.

The solution of these equations is straightforward but lengthy. Here we simply present the solution in a form appropriate for quartz when $\omega\approx\omega_{12}$. Let us define the reduced frequency displacement

$$z=\frac{\omega-\omega_{12}}{|\Omega_{12}|}\ , \tag{15}$$

and the partial polarization $\vec{P}_{mn}(t)$,

$$\vec{P}_{mn}(t)=4\mathrm{Re}[a_m^{*}(t)a_n(t)e^{i\omega_{mn}t}\langle\psi_m|\vec{I}|\psi_n\rangle]\ , \tag{16}$$

where

$$\vec{P}(t)=\sum_{m<n}\vec{P}_{mn}(t)\ .$$

Note that the partial polarization $|\vec{P}_{mn}|$ is the amplitude of the μSR signal near ω_{mn}. The two partial polarizations of interest are $\vec{P}_{12}$ and $\vec{P}_{23}$, given by

$$\vec{P}_{12}=\mathrm{Re}\left\{\langle\psi_1|\vec{I}|\psi_2\rangle a_1^{*}(0)a_2(0)\left[\left[1+\frac{z}{(z^2+1)^{1/2}}\right]^2 e^{i[\omega-(z^2+1)^{1/2}|\Omega_{12}|]t}+\frac{2}{z^2+1}e^{i\omega t}+\left[1-\frac{z}{(z^2+1)^{1/2}}\right]^2 e^{i[\omega+(z^2+1)^{1/2}|\Omega_{12}|]t}\right]\right\}, \tag{17}$$

$$\vec{P}_{23}=2\mathrm{Re}\left\{\langle\psi_2|\vec{I}|\psi_3\rangle a_2^{*}(0)a_3(0)\left[\left[1-\frac{z}{(z^2+1)^{1/2}}\right]e^{i(\omega_{23}-\omega_2^{+})t}+\left[1+\frac{z}{(z^2+1)^{1/2}}\right]e^{i(\omega_{23}-\omega_2^{-})t}\right]\right\}, \tag{18}$$

where

$$\omega_2^{\pm}=\tfrac{1}{2}[z\pm(z^2+1)^{1/2}]\,|\Omega_{12}|\ . \tag{19}$$

Equations (17) and (18) display the expected effects: The transition near ω_{12} splits into three lines at

$$\omega,\omega\pm(z^2+1)^{1/2}|\Omega_{12}|$$

and the transition near ω_{23} splits into two lines at

$$\omega_{23}-\tfrac{1}{2}[z\pm(z^2+1)^{1/2}]\,|\Omega_{12}|\ .$$

TABLE I. Results of DEMUR on quartz. These three data sets show the effects of applying the rf near (a) the lower μSR transition, (b) the midfrequency, and (c) the upper μSR transition. These results correspond to the power spectra shown in Fig. 3.

Data set	Applied rf (MHz) ($H_1=1.0$ G)	Experimental results		Calculated	
		Frequency (MHz)	Amplitude	Frequency (MHz)	Amplitude
a	167.301	166.25±0.025	0.0133±0.0009	166.32	0.0124
		167.24±0.018	0.0187±0.0009	167.30	0.0189
		168.17±0.05	0.0064±0.0009	168.28	0.0072
		179.69±0.034	0.0098±0.0009	179.92	0.0091
		180.84±0.034	0.0100±0.0009	180.90	0.0108
b	173.898	167.11±0.011	0.0288±0.0009	167.05	0.0121
				167.15	0.0167
				173.90	0.0016
		180.60±0.014	0.0233±0.0009	180.55	0.0102
				180.64	0.0131
c	180.510	166.56±0.025	0.0115±0.0010	166.61	0.0116
		167.68±0.03	0.0139±0.0010	167.68	0.0138
		179.39±0.04	0.0081±0.0010	179.45	0.0079
		180.42±0.025	0.0141±0.0010	180.51	0.0139
		181.51±0.05	0.0061±0.0010	181.57	0.0063

TABLE II. Results of DEMUR on quartz. The three DEMUR spectra shown here were all taken with the rf power applied near the upper μSR transition frequency. These results correspond to the power spectra shown in Fig. 4.

Data set	Applied rf (MHz) ($H_1=1.56$ G)	Experimental results Frequency (MHz)	Amplitude	Calculated Frequency (MHz)	Amplitude
a	180.279	166.44±0.017	0.0133±0.0006	166.47	0.0130
		168.09±0.02	0.0114±0.0006	168.08	0.0117
		178.72±0.045	0.0050±0.0006	178.69	0.0054
		180.30±0.015	0.0154±0.0006	180.28	0.0131
		181.84±0.038	0.0061±0.0006	181.92	0.0079
b	180.490	166.07±0.03	0.0117±0.0010	166.43	0.0125
		167.75±0.024	0.0143±0.0010	168.02	0.0135
		178.80±0.048	0.0071±0.0010	178.90	0.0070
		180.39±0.025	0.0138±0.0010	180.49	0.0141
		182.03±0.047	0.0072±0.0010	182.08	0.0070
c	181.517	165.26±0.06	0.0041±0.0006	165.75	0.0054
		167.49±0.01	0.0224±0.0007	167.61	0.0211
		179.63±0.015	0.0161±0.0007	179.65	0.0167
		181.40±0.025	0.0101±0.0007	181.52	0.0095
				183.36	0.0013

The splittings are all equal and proportional to $|\vec{H}_1|$ through Ω_{12}. The amplitude depends on the reduced frequency displacement z. On resonance, $z=0$, the two lines near ω_{23} have equal amplitude, and the two outer lines near ω_{12} have half the amplitude of the center line.

To make a quantitative comparison of our data with the calculation we estimate z from Eqs. (17) and (18) and the observed ratios of the amplitudes in each group of lines. Knowing z, the observed splittings are used to estimate $|\Omega_{ij}|$. The remaining spin-Hamiltonian parameters can be obtained from the no-rf spectrum. With the use of these estimates frequencies and amplitudes of all the observed lines are calculated from a set of coupled equations derived from Eqs. (6) by neglecting all explicit time dependence except that at frequencies $\omega-\omega_{12}$ and $\omega-\omega_{23}$. The calculated amplitudes are normalized to the total experimental amplitude in each group of lines. The estimated parameters are then adjusted and the calculation repeated to obtain the best agreement with the observed spectra.

Tables I and II, corresponding to the Fourier-transform spectra of Figs. 3 and 4, summarize our results. The rf was measured directly, while the rf amplitude was deduced from the DEMUR results. The experimental parameters are the best-fit values of $\omega_i/2\pi$ and a_i from Eq. (1). The calculated parameters are the result of the adjustment procedure described above. In performing this adjustment, an attempt was made to reproduce the observed splittings and amplitudes. Because of calibration differences between the μSR spectrum and the rf counter, the absolute frequencies are in error by as much as 0.3%.

Overall, the agreement with experiment is good. Note in particular that the calculation accurately reproduces the small changes in splitting and the substantial changes in amplitude as ω is varied through resonance (Table II). With the use of these results it would be possible to locate the resonance quite accurately even if the driven transition could not be observed directly.

IV. CONCLUSIONS

We have successfully demonstrated a new double-resonance technique, DEMUR, which is applicable to muoniumlike defects in solids. Using DEMUR, one can study EPR transitions which do not appear directly in the μSR spectrum, thereby obtaining additional clues to the structure of the defect center. The quantitative agreement obtained here provides encouragement to its application to the study of anomalous muonium in silicon, germanium, or diamond.

ACKNOWLEDGMENTS

This work was supported in part by the U. S. Department of Energy through Los Alamos National Laboratory and in part by the National Science Foundation under Grant No. DMR-79-09223.

*Present address: Hewlett-Packard Corp., Palo Alto, California 94304.

[1]J. H. Brewer, K. M. Crowe, F. N. Gygax, and A. Schenck, in *Muon Physics,* edited by V. W. Hughes and C. S. Wu (Academic, New York, 1975), Vol. III, pp. 3–139.

[2]J. H. Brewer and K. M. Crowe, Ann. Rev. Nucl. Part. Sci. 38, 239 (1978).

[3]Proceedings of the 2nd International Topical Meeting on μSR, Section II, edited by J. H. Brewer and P. W. Percival [Hyperfine Interact. 8, 307 (1981)].

[4]T. L. Estle and D. A. Vanderwater, preceding paper, Phys. Rev. B 27, 3962 (1983).

[5]J. H. Brewer, D. S. Beder, and D. P. Spencer, Phys. Rev. Lett. 42, 808 (1979).

[6]J. A. Brown, S. A. Dodds, T. L. Estle, R. H. Heffner, M. Leon, and D. A. Vanderwater, Solid State Commun. 33, 613 (1980).

[7]J. A. Brown, R. H. Heffner, M. Leon, S. A. Dodds, D. A. Vanderwater, and T. L. Estle, Phys. Rev. Lett. 43, 1751 (1979).

[8]D. A. Vanderwater, S. A. Dodds, T. L. Estle, J. A. Brown, R. H. Heffner, M. Leon, and D. W. Cooke, Hyperfine Interact. 8, 823 (1981).